# STUDY OF THE ABSORPTION AND DESORPTION PROCESS OF AN ANTIBIOTIC IN SPHERICAL ACRYLIC POLYMER-BASED HYDROGELS

V. Rojas[(1)(*)], G. Rodriguez[(2)], P. Boschetti[(1,3)], M. Sabino[(1)]

[(1)] Grupo B[5]IDA, Departamento de Química, Universidad Simón Bolívar, Caracas, Venezuela.
[(2)] Laboratorio de superficies, Laboratorio E, Universidad Simón Bolívar, Caracas, Venezuela.
[(3)] Bahlmann Life and Science, Regulatory Affairs & Quality Management Specialist. Hechingen, WD, Deutschland

[(*)] Email: imvicmary@gmail.com.

Received: 15-07-2024 Accepted: 12-09-2024
Published: 27-03-2025

**ABSTRACT**
Acrylic-based hydrogels with spherical geometry were characterized and subjected to a study of absorption/desorption to evaluate the encapsulation and release of a commercial solution of the antibiotic Ciprofloxacin (200 mg/100 ml) at 25 °C. The characterization was performed by means of infrared spectroscopy, macro magnifying glass, scanning electron microscopy and X-ray energy dispersion. Based on the experimental adsorption and desorption results, mass percentage (g/g) and volumetric percentage ($mm^3/mm^3$) curves were constructed for both processes. Additionally, using the mass swelling percentages, diffusivity was analyzed using Fick's Second Law and employing the lattice-Boltzmann computational method (LBM) to simulate the behavior. Consequently, the gels were demonstrated to be superabsorbent, and the effectiveness of the diffusion process in polyacrylic based hydrogels with spherical geometry was verified.

**Keywords**: spherical-hydrogels; acrylic-polymers; diffusion-process; ciprofloxacin; lattice-Boltzmann-method.

## ESTUDIO DEL PROCESO DE ABSORCIÓN Y DESORCIÓN DE UN ANTIBIÓTICO EN HIDROGELES DE GEOMETRÍA ESFÉRICA A BASE DE UN POLÍMERO ACRÍLICO

**RESUMEN**
Se caracterizaron hidrogeles de base acrílica con geometría esférica y se sometieron a un estudio de los procesos de absorción/desorción para evaluar el encapsulamiento y liberación de una solución comercial del antibiótico Ciprofloxacina (200 mg/100 ml) a 25 °C. La caracterización fue realizada mediante espectroscopía infrarroja, macrolupa, microscopía electrónica de barrido y dispersión de energía de rayos X. Luego, a partir de los resultados experimentales de absorción y desorción obtenidos, se realizaron las curvas en porcentaje de masa (g/g) y porcentaje volumétrico ($mm^3/mm^3$) para ambos procesos. Además, con los porcentajes másicos de hinchamiento, se analizó la difusividad mediante la segunda Ley de Fick y empleando el método computacional de lattice-Boltzmann (LBM) para realizar una simulación del comportamiento. A partir de esto, se demostró que los geles son superabsorbentes y se comprobó la efectividad del proceso de difusión en hidrogeles con geometría esférica a base de un polímero acrílico.

**Palabras claves**: hidrogeles-esféricos; polímeros-acrílicos; procesos-difusivos; ciprofloxacina, método-lattice-Boltzmann.

## INTRODUCTION

Hydrogels are three-dimensional polymeric networks that swell in aqueous solutions while maintaining their structural integrity. This swelling behavior is attributed to the dissolution of hydrophilic polymer molecules in water and the presence of charged polar groups that impart hydrophilicity to the gel [1]. The swollen equilibrium state arises from a balance between osmotic driving forces that draw water into the hydrophilic polymer possessing a 3D molecular crosslinking (chemical, physical, or interpenetrated) and the forces exerted by the polymer chains to resist the expansion caused by water diffusion [2].

The characteristic properties of hydrogels, such as water expansion (swelling), high water content, elastic nature

similar to natural tissues, and non-toxicity, have enabled them to find wide-ranging applications in various fields, including pharmaceutical [3-5], biomedical [3-7], bioengineering and biotechnology [9-10] and agricultural applications [10]. Driven by the wide-ranging applications of hydrogels, researchers have been actively investigating the diffusion mechanism of these versatile materials.

The swelling kinetics of hydrogels can be elucidated using Fick's Second Law and further explored through computational modeling applying the lattice-Boltzmann method (LBM) [11] for spherical geometry, where diffusivity in a specific direction ($D_r$) is an equation dependent on the water concentration ($C(t)$), according to the dependence of the Fujita exponential model [11]:

$$D_r = D_{eq} \cdot \exp\left(-\beta\left(1-\frac{C(t)}{C_{eq}}\right)\right) \quad (1)$$

Simultaneously, this exponential depends on the dimensionless constant $\beta$ the equilibrium diffusivity ($D_{eq}$), and the mass concentration of water in thermodynamic equilibrium ($C_{eq}$).

Since diffusivity varies with water concentration as described by Equation (1), a Multiple Relaxation Time (MRT) Lattice Boltzmann Method (LBM) formulation is advantageous. This approach enables the independent estimation of relaxation coefficients for each moment. [11] Considering the promising potential of hydrogels as drug delivery systems, this study delves into the diffusion behavior of Ciprofloxacin, a broad-spectrum antibiotic belonging to the fluoroquinolone family. Ciprofloxacin is commonly prescribed to treat bacterial infections.

## MATERIALS AND METHODS

The spherical hydrogel samples used in this study were commercially sourced, primarily for plant hydration in hydroponics. These commercial beads for agricultural applications are usually synthesized from acrylate-based polymers [12]. A 200 mg/100 mL Ciprofloxacin commercial solution was also implemented. See table 1.

**Table 1**. Chemical structures of the materials used

| Material | Name | Structure |
|---|---|---|
| Hydrogel* | Sodium polyacrylate | 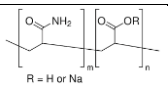 |
| Drug substance | Ciprofloxacin | 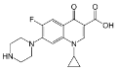 |

* Potential structure of the spheres used

*Characterization*

To characterize the morphology of xerogel and composition, some analytical techniques were employed. For characterization by FTIR-ATR spectroscopy, a Thermo Scientific Nicolet iS10 device with Smart iTR accessory (ZnSe crystal) was used, at a 4 $cm^{-1}$ resolution and 32 scans. The absorbance spectrum was carried out from 600 to 4000 $cm^{-1}$. While the treatment of the samples prior to introduction to the equipment required drying in an oven to remove traces of moisture in the xerogel spheres.

The Scanning Electron Microscopy (SEM) required a thin gold coating on the xerogel samples, using a Blazers-SCD-03 sputter coater, prior to introduction into the JEOL – JSM-6390 scanning electron microscope at 15 KV. Also, the Energy Dispersion X-ray (EDX) technique was performed. The macro magnifying employed was an Olympus SZ61 microscope fitted with a Hitachi CCD Color Digitizer model KP-D20BU.

*Swelling and deswelling studies*

Absorption and desorption experiments were conducted at 25°C in a 200 mg/100 mL ciprofloxacin solution. The hydrogel beads were weighed using a U.S. Solid JFDBS00008 analytical balance with an accuracy of (±0.0001) g. Starting from time zero (xerogel), the

diameter and mass changes of the beads were measured at regular time intervals until equilibrium was reached.

For desorption, the beads were removed from the aqueous medium and placed on a fine mesh at 25 °C. The mass of the samples was measured at short time intervals until a final constant weight value was obtained. Based on the recorded diameters and masses for each sample and at different times, swelling and deswelling isotherms were constructed for hydrogel as a function of volume and mass.

*Computational Simulations*

The LBM utilizes dimensionless length and mass parameters, independently calculating mass sample concentration estimates at each time step without requiring volume data. This offers a significant advantage over other numerical methods. [11]

The diffusion coefficient, computed using Equation (1), was incorporated into the relaxation coefficients of LBM, for two- and three-dimensional simulations, respectively. The equilibrium diffusion coefficient, optimized to fit with experimental data, was employed in conjunction with the Fujita dimensionless constant $\beta$ and the preceding time step's water concentration. Lastly, to ensure numerical accuracy, discretization errors for simulations of hydrogel samples were estimated using the Grid Convergence Index (GCI) method, which relies on generalized Richardson extrapolation to quantify numerical uncertainty by comparing solutions across different grid resolutions [12].

## RESULTS AND DISCUSSION

*Characterization*

The ATR-FTIR spectrum revealed the presence of various functional groups characteristic of the hydrogel's composition and their acrylic nature (see Figure 1). The band around 3341 $cm^{-1}$ indicates the presence of residual water, a common characteristic of highly hydrophilic hydrogels. The band at 2935 $cm^{-1}$ corresponds to the stretching vibrations of carbon atoms (sp, sp2, and sp3) present in the hydrogel's structure. A peak at 1651 $cm^{-1}$ confirms the presence of a carbonyl (C=O) group, this band also overlaps with the OH bending vibration of water. The band at 1548 $cm^{-1}$ is attributed to the stretching vibration of the carboxylate ($-COO^-$) group, while the bands at 1451 and 1403 $cm^{-1}$ are assigned to the C-N bond of the acrylamide unit; which indicates the nature of an acrylic polymer [13]. Consulting the spectral library offered by the FTIR equipment software, it was possible to verify that the base polymer of the hydrogel corresponds likely to copolymer acrylamide-co-acrylate.

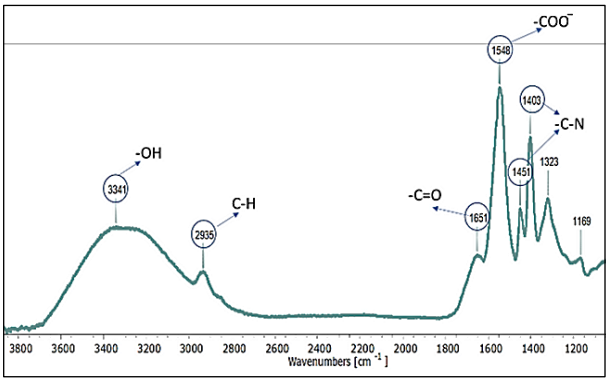


**Fig. 1.** FTIR spectra of polyacrylamide hydrogels.

The morphology and dimensions of the hydrogel beads were examined using macro magnifying glass and SEM. As illustrated by SEM in Figure 2, the xerogel beads exhibited a diameter around 2 mm.

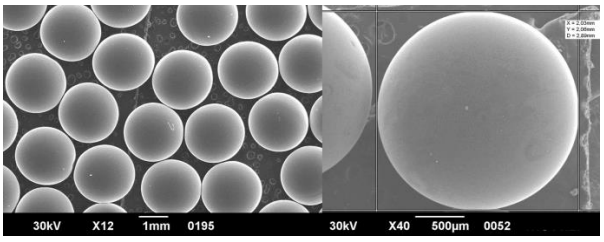


**Fig. 2.** SEM on a set of dry beads or xerogel.

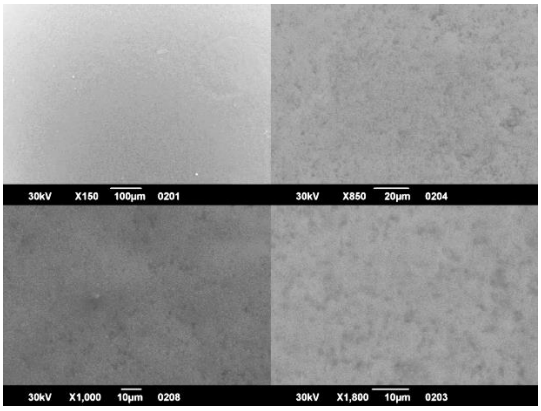


**Fig. 3.** SEM of the sample structure with magnifications of X150, X830, X1000 and X1800.

Higher magnification SEM images (X150, X850, X1000, and X1800) revealed a smooth surface morphology with slight surface roughness, see Figure 3.

EDX analysis, from SEM equipment, was performed to determine the elemental composition of the hydrogel beads. The semi-quantitative analysis revealed the presence of the following elements, see table 2:

**Table 2.** Elements found with EDX, expressed in weight %

| Element | Weight % |
|---|---|
| C (*) | 54.50 |
| O | 36.68 |
| Na | 8.92 |

(*) Nitrogen could be mask by high % of carbon

These elemental compositions are consistent with the presence of carboxylate groups, suggesting the presence of a copolymer acrylamide-co-acrylate sodium xerogel. Although the nitrogen signal was not clear in the semiquantitative EDX analysis, this signal could be masked by the coarse carbon signal [14].

*Swelling process*

The volumetric adsorption profile (% v/v) exhibited an increasing trend, with the maximum swelling percentage reaching 1463 % ($mm^3/mm^3$), as shown in Figure 4.

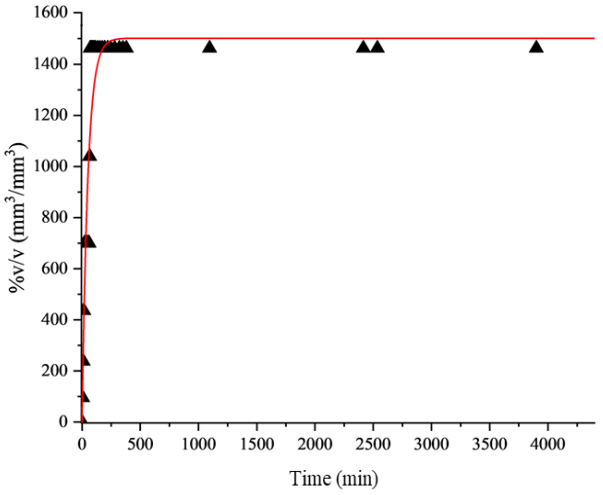


**Fig. 4.** Swelling isotherm in terms of %v/v vs. time (minutes) at 25°C.

The mass swelling profile (%H, m/m) attained a value of 1046 % (g/g) and served as an input parameter for the LBM-MRT absorption simulations. These simulations yielded results consistent with diffusion in thermodynamic equilibrium, as shown in Figure 5.

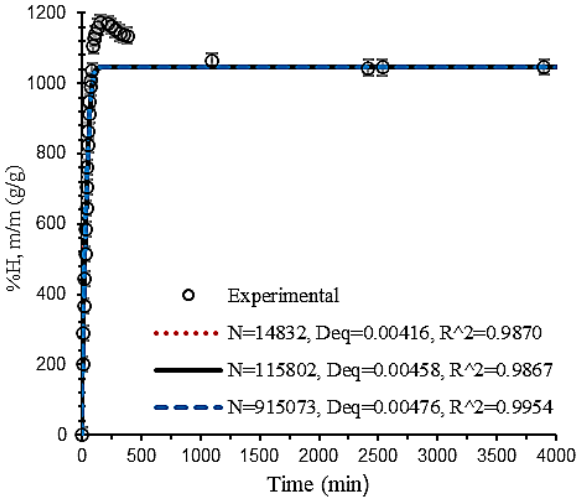


**Fig. 5.** Swelling curve (%H) in terms of % m/m vs. time (min) at 25 °C, including comparison of experimental data with the LBM for each number of lattice elements (coarse, medium and fine)

The GCI was determined for the finest lattice to assess solution accuracy, and the achieved Fujita dimensionless constant is $\beta$=2.5. The values accomplished for the sample are in agreement with experimental equilibrium data, with $R^2$=0.9954 for a fine lattice type. See table 3:

**Table 3.** GCI discretization error for different types of lattices: coarse ($N_y$ = 30), medium ($N_y$ = 60) and fine ($N_y$ = 120) for Ciprofloxacin solution at 25 °C.

| $N$ | $N_y$ | $D_{eq}$, mm²/min | $R^2$ | $D_{eq}^*$ | $GCI_{fine}$ |
|---|---|---|---|---|---|
| 14832 | 30 | 0.00416 | 0.9870 | | |
| 115802 | 60 | 0.00458 | 0.9866 | | |
| 915073 | 120 | 0.00476 | 0.9954 | 0.004895 | 3.545 % |

Upon reaching equilibrium, a macro magnifying glass observation revealed that the swollen samples attained a diameter of 5 mm (with a volume of 65.45 $mm^3$) and exhibited a whitish coloration, which indicates the presence of the antibiotic within the material, as presented in Figure 6.

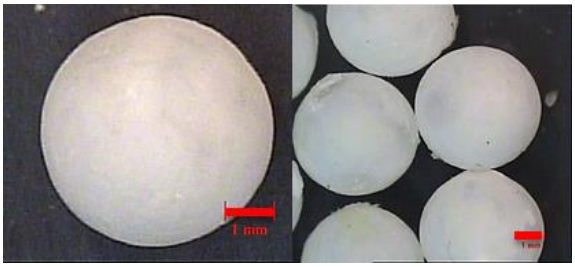


**Fig. 6.** Macroscopic observation of the swollen hydrogel

*Deswelling process*

The volumetric desorption curve (% v/v) exhibited a value of 12.5 % $mm^3/mm^3$, as illustrated in Figure 7. Similarly, the mass desorption percentage %D (m/m) reached 13.43 % (g/g), shown inside the same figure.

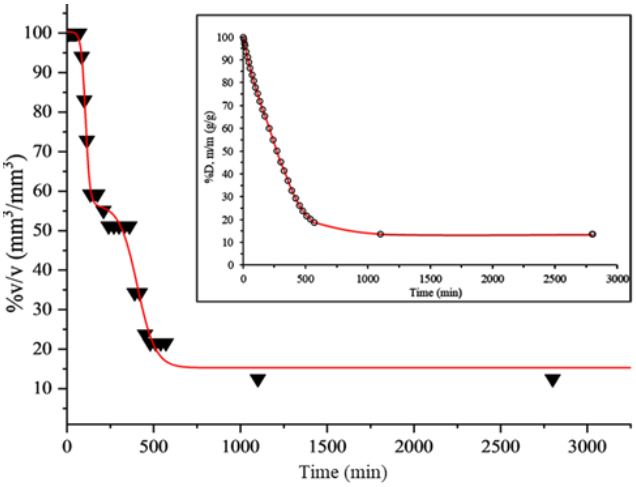


**Fig. 7.** Deswelling isotherm in terms of %v/v vs. time (minutes). Inside: Deswelling curve (%D) in terms of mass (g/g) vs. time (minutes). Experience at 25 °C.

Once the desorption was completed, the samples were subjected to final observations using a magnifying glass and SEM to assess their condition after the entire sorption process. It was noted that the white coloration persisted in the samples even after complete deswelling. This indicates a change in its refractive index which can be attributed to the presence of drug remains within the xerogel and the rough texture, that mean the structure lost its perfectly spherical geometry and exhibited a wrinkled and amorphous appearance, as illustrated in Figure 8.

Besides this, semi-quantitative EDX analysis revealed the presence of the following elements, see table 4.

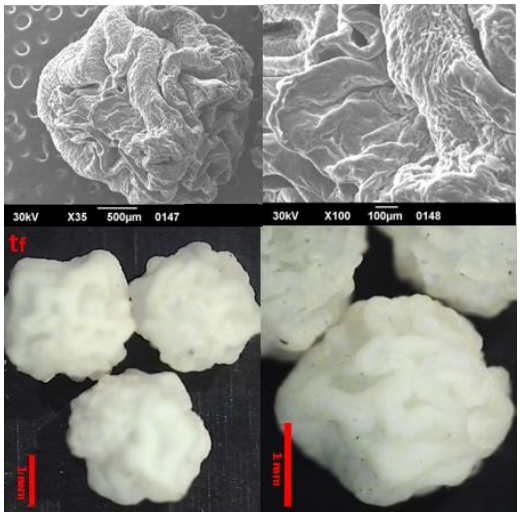


**Fig. 8.** Dehydrated samples after isothermal deswelling. Down: Macroscopic observation. Up: SEM observation.

**Table 4.** Elements found with EDX after the deswelling process, expressed in weight %.

| Element | Weight % |
|---|---|
| O | 50.96 |
| F | 22.95 |
| Na | 11.07 |
| Cl | 15.02 |

This confirms what was seen in the previous figure, which also explains the percentage of retention obtained from the isotherms, indicating the fluorine presence that remains ciprofloxacin after the deswelling of the hydrogels. In this way is confirming the presence of residues of the ciprofloxacin molecule inside the polymeric networks.

## CONCLUSIONS

This study investigated the characteristics and behavior of polyacrylic hydrogels for potential drug delivery applications. Morphological analysis using SEM and magnifying glass revealed that the xerogel exhibited a uniform spherical shape with a diameter of 2 mm and a smooth surface. FTIR-ATR and EDX confirmed the composition of the hydrogel base material.

The hydrogel exhibited a remarkable absorption capacity, with maximum volumetric and gravimetric swelling values reaching 1463 % (v/v) and 1046 % (m/m), respectively. Importantly, the hydrogel also demonstrated efficient desorption properties, with volumetric and gravimetric desorption percentages of 12.5 % (v/v) and 13.43 % (m/m), indicating good reversibility. While EDX analysis verified the presence of the drug within the material even after desorption.

Additionally, computational simulations employing the Lattice-Boltzmann method yielded results consistent with the experimental mass data.

These findings highlight the promising potential of these hydrogels as drug delivery vehicles due to their favorable properties, including their superabsorbent capacity, drug retention capability and ability to control release this drug.

## ACKNOWLEDGEMENT

Laboratorio de Carbón, Lab-B. Laboratorio de Superficies y MEB, Lab-E. Universidad Simón Bolívar, Caracas, Venezuela

## REFERENCES

[1] Alam, M. M., Mina, M. F., Akhtar, F. (2003) "Swelling and Hydration Properties of Acrylamide Hydrogel in Distilled Water" *Polym. -Plast. Technol. Eng* 42(4), 533-542.

[2] Wu, J., Xue, W., Yun, Z., Liu, Q., Sun, X. (2024) "Biomedical applications of stimuli-responsive "smart" interpenetrating polymer network hydrogels." *Materials Today Bio*, 100998.

[3] Malmonge, S. M., Barboza, J. K., Castro, A., Ferreira, K., Sabino, M. A. (2023) "Natural Hydrogels for Drug Delivery Systems" *Current Trends in Biomedical Engineering*, pp. 149-167.

[4] Nguyen, H. T., Truong, B. C., Dang, X. C. (2023). "Polymer-Based Hydrogels Applied in Drug Delivery: An Overview" *Gels* 9:5, 523.

[5] Bindu Sri, M., Ashok, V., Arkendu, C. (2012) "A Review on Hydrogels as Drug Delivery in the Pharmaceutical Field" *Int. J. Pharm. Chem. Sci* 1(2), 642–661.

[6] Caló, E., Khutoryanskiy, V. V. (2015) "Biomedical applications of hydrogels: A review of patents and commercial products" *Eur. Polym. J*, 65, 252–267.

[7] Chakrapani, G., Zare, M., & Ramakrishna, S. (2022) "Intelligent hydrogels and their biomedical applications" *Materials Advances*, 3, 7757.

[8] Wei, S.-Y., Chen, T.-H., Kao, F.-S., Hsu, Y.-J., Chen, Y.-C. (2022) "Strategy for improving cell-mediated vascularized soft tissue formation in a hydrogen peroxide-triggered chemically-crosslinked hydrogel" *J. Tissue Eng*., 13, 1–20.

[9] Yang, J., Wang, S. (2023) "Polysaccharide-Based Multifunctional Hydrogel Bio-Adhesives for Wound Healing: A Review" *Gels*, 9, 138.

[10] Kratochvílová, R., Kráčalík, M., Smilková, M., Sedláček, P., Pekař, M., Bradt, E., Smilek, J., Závodská, P., Klučáková, M. (2023) "Functional Hydrogels for Agricultural Application" *Gels*, 9, 590.

[11] Boschetti, P. J., Toro, D. J., Ontiveros, A., Pelliccioni, O., Sabino, M. A. (2022). "Lattice Boltzmann method simulations of swelling of cuboid-shaped IPN hydrogel tablets with experimental validation." *Heat and Mass Transfer*, 58(5), 763–77.

[12] Ortega-Torres A.E., Flores L.B., Guevara-González R.G., Rico-García E., Martín Soto-Zarazúa G. (2021) "Hidrogel acrilato de potasio como sustrato en cultivo de pepino y jitomate" *Rev. Mex. Cienc. Agríc*.11, 6.

[13] Spagnol, C., Rodrigues, F. H. A., Neto, A. G. V. C., Pereira, A. G. B., Fajardo, A. R., Radovanovic, E., Rubira, A. F., Muniz, E. C. (2012). "Nanocomposites based on poly(acrylamide-co-acrylate) and cellulose nanowhiskers." *Eur. Polym. J.*, *48*(3), 454–463.

[14] Terzano, R., Denecke, M. A., Falkenberg, G., Miller, B., Paterson, D., Janssens, K. (2019). "Recent advances in analysis of trace elements in environmental samples by X-ray based techniques (IUPAC Technical Report)". *Pure Appl. Chem.*, *91*(6), 1029–106.